

Synthesis and characteristics of nanostructured $\text{Li}(\text{Co}_{1/3}\text{Ni}_{1/3}\text{Mn}_{1/3})\text{O}_2$ cathode material prepared at 0 °C

C. Deng · S. Zhang · B. Wu · S. Y. Yang · H. Q. Li

Received: 16 March 2009 / Revised: 13 May 2009 / Accepted: 26 May 2009 / Published online: 9 June 2009
© Springer-Verlag 2009

Abstract Special synthetic conditions at 0 °C were used to prepare nanostructured $\text{Li}[\text{Ni}_{1/3}\text{Co}_{1/3}\text{Mn}_{1/3}]\text{O}_2$ via chemical coprecipitation synthesis. The precursor preparation shows platelet shape with thickness of 10 nm and width of 100 nm. After calcination, the particles change to spherical or rectangle shape with a size of 100–200 nm. The nanostructured $\text{Li}[\text{Ni}_{1/3}\text{Co}_{1/3}\text{Mn}_{1/3}]\text{O}_2$ shows a well-ordered layered hexagonal lattice with low cation mixing. Galvanostatic testing showed good electrochemical properties and high rate capability, which may be due to its unique morphological and structural characteristics. Synthesis at 0 °C effectively prevented growth of the precursor particles and produced nanosize $\text{Li}[\text{Ni}_{1/3}\text{Co}_{1/3}\text{Mn}_{1/3}]\text{O}_2$, which gave improvement in high rate performance and favoring the future use of this cathode material for high power applications.

Keywords Nanostructure · Chemical synthesis · Oxides · Electrochemical properties

Introduction

Rechargeable lithium-ion batteries (LIB) are becoming increasingly important as power sources for portable

consumer electronics. LiCoO_2 has been widely used as the cathode material for commercial lithium-ion battery because of its easy synthesis and stable discharge capacity. However, the high cost, limited discharge capability, and toxicity of LiCoO_2 inhibit its further application in high power and price-sensitive fields, such as electric vehicles [1, 2]. Therefore, many efforts have been made to find alternative to LiCoO_2 , which should have such characteristics as high specific energy, high specific power, safety, together with low cost.

$\text{Li}[\text{Ni}_y\text{Co}_{1-2y}\text{Mn}_y]\text{O}_2$, a solid solution of LiCoO_2 , LiNiO_2 , and LiMnO_2 , was introduced by Z. H. Lu and J. R. Dahn as a candidate cathode material for LIB [3–6]. $\text{Li}[\text{Ni}_{1/3}\text{Co}_{1/3}\text{Mn}_{1/3}]\text{O}_2$ is a special case of the $\text{Li}[\text{Ni}_y\text{Co}_{1-2y}\text{Mn}_y]\text{O}_2$ family, in which y is 1/3. $\text{Li}[\text{Ni}_{1/3}\text{Co}_{1/3}\text{Mn}_{1/3}]\text{O}_2$ has layered hexagonal structure and the valence states of Ni, Mn, and Co are divalent, tetravalent, and trivalent, respectively. During the electrochemical charge/discharge process, the tetravalent Mn is inactive, which plays an important role in stabilizing the host structure and favoring the cycling performance [7]. Therefore, $\text{Li}[\text{Ni}_{1/3}\text{Co}_{1/3}\text{Mn}_{1/3}]\text{O}_2$ has many advantages such as high reversible capacity, good cycle performance, and safety and has been considered as the best candidate of cathode material for the lithium ion battery [8].

For high power applications such as hybrid electric vehicles, the properties of high rate capability and cycle stability are very important. High rate capability largely depends on the morphology and particle size of the active material in the electrodes. In LIB, the diffusion rates of lithium ion and electrons in the active cathode material are limited, which further limit the rate capability of the battery. Nanostructured particles greatly reduce the diffusion distances of the lithium ion and electron and effectively improve the high rate capability of active material [9].

C. Deng (✉) · B. Wu · H. Q. Li
College of Chemistry and Chemical Engineering,
Provincial Key Lab for Nano-functionalized Materials
and Excited State, Harbin Normal University,
Harbin, Heilongjiang 150025, China
e-mail: chaodeng2008@yahoo.cn

S. Zhang (✉) · S. Y. Yang
College of Materials Science and Chemical Engineering,
Harbin Engineering University,
Harbin, Heilongjiang 150001, China
e-mail: senzhang@hrbeu.edu.cn

However, synthesis of the mixed transition metal oxide, $\text{Li}[\text{Ni}_{1/3}\text{Co}_{1/3}\text{Mn}_{1/3}]\text{O}_2$, with nanometer-size particles has not proved easy. The transition metal component often saturates and produces such impurities as NiO , Co_3O_4 , and MnO_2 in the material. Moreover, it is difficult to control the nanoparticle size of $\text{Li}(\text{Ni}_{1/3}\text{Mn}_{1/3}\text{Co}_{1/3})\text{O}_2$ [10]. Therefore, selection of an appropriate synthetic method is very critical in obtaining a nanostructured material with high purity.

In this paper, the nanostructured $\text{Li}(\text{Ni}_{1/3}\text{Mn}_{1/3}\text{Co}_{1/3})\text{O}_2$ particles were prepared under a special synthetic condition, namely at 0°C via a hydroxide coprecipitation method. With this novel synthetic process, nanostructured $\text{Li}(\text{Ni}_{1/3}\text{Mn}_{1/3}\text{Co}_{1/3})\text{O}_2$ with high purity, layered structure, and improved rate capability was synthesized. The structure, morphology, and electrochemical characteristics of the nanostructured materials obtained were studied in detail.

Experimental

Synthesis of nanostructured $\text{Li}[\text{Ni}_{1/3}\text{Co}_{1/3}\text{Mn}_{1/3}]\text{O}_2$

All the coprecipitation reaction took place in an ice environment. The reactor was kept in the ice–water mixing environment and the reaction solution was maintained at 0°C . The aqueous solution of NiSO_4 , CoSO_4 , and MnSO_4 (cationic ratio of $\text{Ni}/\text{Co}/\text{Ni}=1:1:1$) with a concentration of $2\text{ mol}\cdot\text{L}^{-1}$ was pumped into continuous stirred tank reactor under nitrogen atmosphere. At the same time, NaOH solution of $2\text{ mol}\cdot\text{L}^{-1}$ and NH_4OH of $0.36\text{ mol}\cdot\text{L}^{-1}$ were also separately fed into the reactor. The reaction solution was kept at 0°C with continuously stirring for 10 h and its pH value was carefully controlled. The precipitated powder was alternately filtered and washed with ethanol and water (the temperature of 0°C) three times, and then it was dried in a vacuum oven at room temperature for 24 h.

The precursor obtained was pressed into pellets. The pellets were calcined at 500°C for 5 h and were subsequently ground. The powder obtained was mixed with LiOH (the molar ratio of $\text{Li}/(\text{Mn} + \text{Co} + \text{Ni})$ was 1.10) using a ball mill and then the powder was pressed into pellets. Finally, pellets were remade and calcined at 800°C for 12 h in air.

Measurements

Powder X-ray diffraction (XRD) employing $\text{Cu K}\alpha$ radiation was used to identify the crystalline phases of the powders prepared. The morphology was observed with a scanning electron microscope (SEM) and a transmission

electron microscope (TEM). The chemical composition was determined with atomic absorption spectroscopy (AAS).

Electrochemical measurements were performed using a 2,032 coin cells composed of a $\text{Li}[\text{Ni}_{1/3}\text{Co}_{1/3}\text{Mn}_{1/3}]\text{O}_2$ cathode and a lithium metal anode separated by a microporous polyethylene film. The cathode was prepared by mixing the active material with conductive carbon black and polyvinylidene fluoride in a weight ratio of 80:10:10. The mixture was pressed onto aluminum foil and then dried under vacuum at 90°C for 10 h. Then, the electrode was rolled, and a circular electrode was cut out. The laboratory cell was assembled in an argon-filled glove box, and the electrolyte consisted of 1 M $\text{LiPF}_6\text{-EC/DMC}$ (1:1 v/v). The electrochemical properties were measured with BTS-2000 Neware Battery Testing System (made in Shenzhen City, Guangdong Province, China), and the cells were tested at $32\text{ mA}\cdot\text{g}^{-1}$ between 2.8 to 4.4 V.

Results and discussions

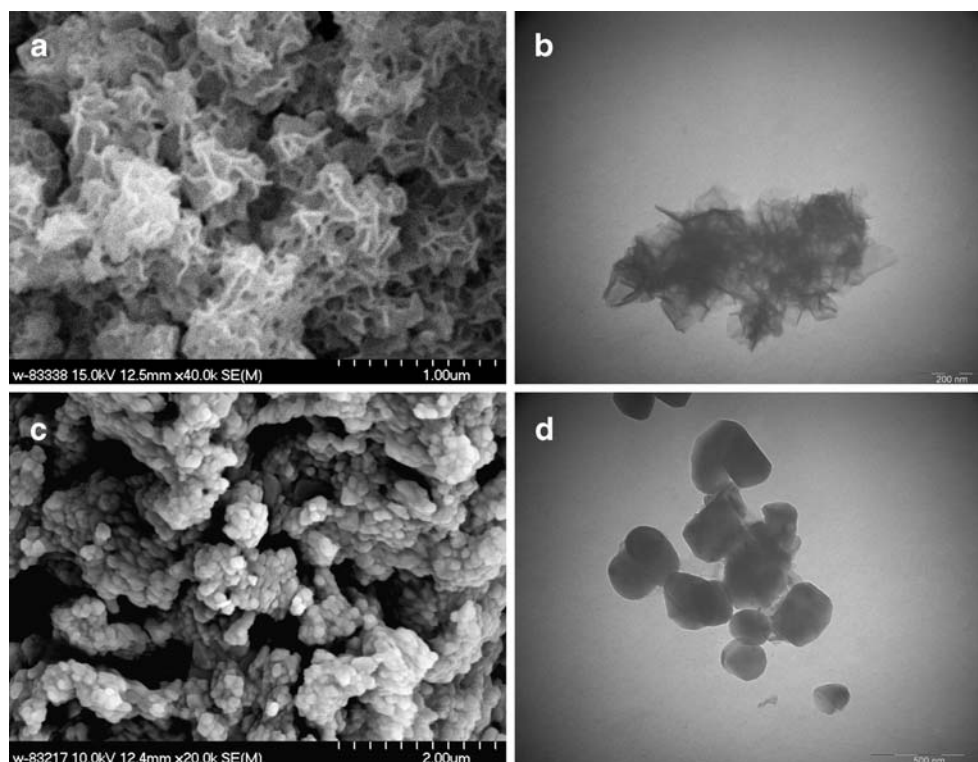
Particle morphology

The chemical composition of the prepared sample was determined by AAS. The ratio of $\text{Li}/\text{Ni}/\text{Mn}/\text{Co}$ was 1.03:0.34:0.33:0.32, which is in good agreement with the expected composition. Figure 1 shows the SEM and TEM images of the precursor and final $\text{Li}(\text{Ni}_{1/3}\text{Mn}_{1/3}\text{Co}_{1/3})\text{O}_2$ product. The precursor particles had the shape of thin platelets in the nanometer-size range. The thickness of the platelets was about 10–20 nm, and the lateral length of the platelets was in the range of 100 nm (Fig. 1a, b). After calcination, the particles of the $\text{Li}(\text{Ni}_{1/3}\text{Mn}_{1/3}\text{Co}_{1/3})\text{O}_2$ material changed to spherical or rectangular shape in the 100–200 nm size range (Fig. 1c, d).

The XRD pattern of the $\text{Li}(\text{Ni}_{1/3}\text{Mn}_{1/3}\text{Co}_{1/3})\text{O}_2$ powders prepared is shown in Fig. 2. The figure identified that the sample has typical hexagonal $\alpha\text{-NaFeO}_2$ structure (space group—166, $R\text{-}3m$) and no secondary phase was observed. In the XRD pattern, the integrated peak splits of (006)/(102) and (018)/(110) are known to be an indicator of layered structure [11]. As seen in the figure, clear peak splits of (006)/(102) and (018)/(110) are observed, which indicated the formation of a highly ordered layer structure for $\text{Li}[\text{Ni}_{1/3}\text{Co}_{1/3}\text{Mn}_{1/3}]\text{O}_2$.

In $\text{Li}[\text{Ni}_{1/3}\text{Co}_{1/3}\text{Mn}_{1/3}]\text{O}_2$, the radius of Ni^{2+} is close to that of Li^+ . A partial interchange of occupancy of Li and transition metal ions among the sites would give rise to disordering in the structure called “cation mixing”. Cation mixing is known to degrade the electrochemical performance of layered compound. The integrated intensity ratio of I_{003}/I_{104} (R) is sensitive to the degree of cation mixing [12]. Researchers often used this intensity ratio to indicate

Fig. 1 Images of prepared precursor and final $\text{Li}(\text{Ni}_{1/3}\text{Mn}_{1/3}\text{Co}_{1/3})\text{O}_2$ product. SEM (a) and TEM (b) images of precursor and SEM (c) and TEM (d) images of $\text{Li}(\text{Ni}_{1/3}\text{Mn}_{1/3}\text{Co}_{1/3})\text{O}_2$



the cation mixing of the layered structure [13]. Generally, $R < 1.2$ is an indication of undesirable cation mixing [14]. A value of $R = 1.33$ was obtained for the prepared $\text{Li}[\text{Ni}_{1/3}\text{Co}_{1/3}\text{Mn}_{1/3}]\text{O}_2$, which indicated a low degree of cation mixing in the structure. Therefore, good electrochemical performance would be expected for the $\text{Li}[\text{Ni}_{1/3}\text{Co}_{1/3}\text{Mn}_{1/3}]\text{O}_2$ prepared.

The lattice parameters were obtained from the XRD data of Fig. 2. The lattice parameter, a , is related to average metal–metal intraslab distance; the lattice parameter, c , is related to the average metal–metal interslab distance; and the trigonal

distortion, c/a , is related to the hexagonal structure disorder. For layered compounds, a higher value of c/a is desirable for better hexagonal structure [15]. The hexagonal lattice parameter of the $\text{Li}[\text{Ni}_{1/3}\text{Co}_{1/3}\text{Mn}_{1/3}]\text{O}_2$ prepared were determined to be $a = 2.8609 \text{ \AA}$ and $c = 14.2231 \text{ \AA}$. These data match well with the values observed in other work [12, 16]. The value of $c/a = 4.972$ shows that a well-defined hexagonal structure is formed. All the above results confirm that the $\text{Li}[\text{Ni}_{1/3}\text{Co}_{1/3}\text{Mn}_{1/3}]\text{O}_2$ powder prepared have well-defined layered hexagonal structure.

The electrochemical properties of the $\text{Li}[\text{Ni}_{1/3}\text{Co}_{1/3}\text{Mn}_{1/3}]\text{O}_2$ material prepared were tested and the results are shown in Figs. 3, 4, and 5. Figure 3 shows the charge/discharge curves of the product during cycling at a constant current density of $32 \text{ mA}\cdot\text{g}^{-1}$ (0.2 C) between 2.8 and 4.4 V versus Li at $30 \text{ }^\circ\text{C}$. The cathode material prepared shows monotonic voltage and capacity variations. The initial charge and discharge capacities were 208.7 and $171.8 \text{ mAh}\cdot\text{g}^{-1}$, respectively, and the coulombic efficiency was 82.3% for the initial cycle.

The changes of discharge capacity and coulombic efficiency during cycling are shown in Fig. 4. The discharge capacity deteriorates slightly on cycling and the coulombic efficiencies of the subsequent cycles are all above 97%. The material shows stable cycling properties and a capacity of $162.5 \text{ mAh}\cdot\text{g}^{-1}$ is obtained after 50 cycles.

Although the above results demonstrate the good electrochemical performance at moderate rates, the impor-

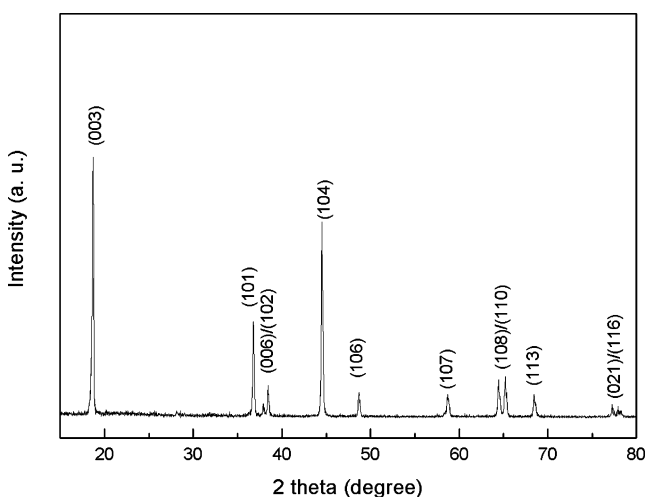


Fig. 2 XRD pattern of $\text{Li}[\text{Ni}_{1/3}\text{Co}_{1/3}\text{Mn}_{1/3}]\text{O}_2$ cathode material

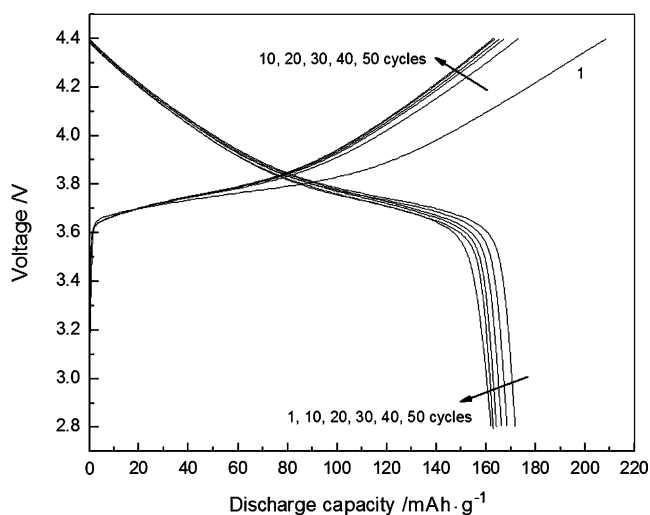


Fig. 3 Charge and discharge curves of the $\text{Li}[\text{Ni}_{1/3}\text{Co}_{1/3}\text{Mn}_{1/3}]\text{O}_2$ preparation over 50 cycles at $32 \text{ mA}\cdot\text{g}^{-1}$ (0.2 C)

tance of high power applications points to an investigation of the high rate performance of this material. Figure 5 shows the different discharge rates capacities of the $\text{Li}[\text{Ni}_{1/3}\text{Co}_{1/3}\text{Mn}_{1/3}]\text{O}_2$ electrode between 2.8 and 4.4 V. The nanostructured cathode material maintains its discharge capacity at high rates. Especially, the discharge capacity obtained at the 4 C rate is 84.2% of that at 0.2 C, which indicates the good high rate performance of the material prepared.

The nanoparticle electrode material showed excellent cycling properties at both moderate and high rates. Its good rate capability is probably due to decreased particle size and improved morphology. For the material prepared by conventional hydroxide coprecipitation, the particle size is often several microns, which results in lower specific surface area and porosity of the electrode. During high current charge and discharge process, the Li ion in bulk lattice of such particles cannot rapidly diffuse to their

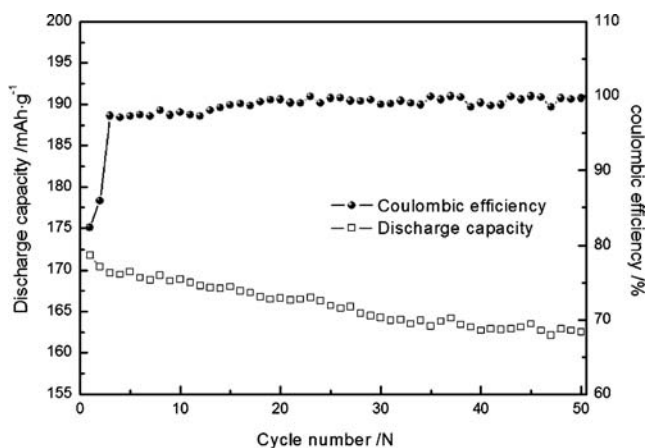


Fig. 4 Changes of discharge capacity and coulombic efficiency of the $\text{Li}[\text{Ni}_{1/3}\text{Co}_{1/3}\text{Mn}_{1/3}]\text{O}_2$ preparation over 50 cycles at $32 \text{ mA}\cdot\text{g}^{-1}$ (0.2 C)

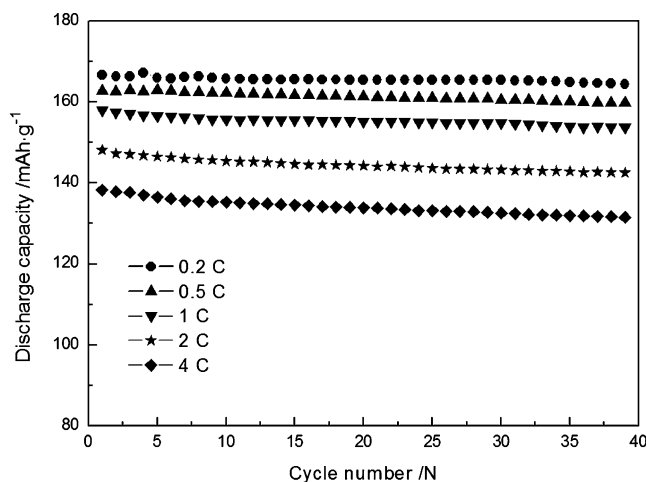


Fig. 5 Discharge capacity of the $\text{Li}[\text{Ni}_{1/3}\text{Co}_{1/3}\text{Mn}_{1/3}]\text{O}_2$ preparation at different discharge rates from 0.2 to 4 C

surfaces because of the long diffusion pathway, resulting in low rate capability. In this work, the preparative coprecipitation process was performed at 0°C , which effectively prevents the growth and aggregation of the primary particle, giving high purity nanostructured material. In this case, the interface area between the electrolyte and the active material is relatively large and the diffusion path of lithium ion from bulk to surface is relatively short. The nanostructured $\text{Li}[\text{Ni}_{1/3}\text{Co}_{1/3}\text{Mn}_{1/3}]\text{O}_2$ powder shows superior high rate capability compared with conventional microsize material.

Conclusion

Nanostructured $\text{Li}[\text{Ni}_{1/3}\text{Co}_{1/3}\text{Mn}_{1/3}]\text{O}_2$ particles were synthesized in an ice environment via a coprecipitation method. Their morphology, structure, and electrochemical performance were characterized using SEM, TEM, XRD, and galvanostatic charge/discharge testing. SEM and TEM images show the synthesized precursor had a platelet particle shape with the thickness of about 10–20 nm. After calcination, the particles change to a spherical or rectangle shape with a size of 100–200 nm. Structural analysis showed that the $\text{Li}[\text{Ni}_{1/3}\text{Co}_{1/3}\text{Mn}_{1/3}]\text{O}_2$ prepared had a well-defined hexagonal layered structure with only a small amount of cation mixing. Good electrochemical properties and superior high rate capability were obtained, which probably result from the unique morphological characteristics of the material, favoring it for high power applications.

Acknowledgment This work was supported by the Development Program for Outstanding Young Teachers in Harbin Normal University (KGB200805) and Postdoctoral Foundation of Heilongjiang Province, China.

References

1. Andersson AM, Abraham DP, Haasch R, Maclaren S, Liu J, Amine K (2002) *J Electrochem Soc* 149:A1358. doi:10.1149/1.1505636
2. Amine K, Chen CH, Liu J, Hammond M, Jansen A, Dees D, Bloom I, Vissers D, Henriksen G (2001) *J Power Sources* 97–98:684. doi:10.1016/S0378-7753(01)00701-7
3. Lu ZH, Dahn JR (2005) US Patent No. 6964828
4. Lu ZH, Dahn JR (2006) US Patent No. 7078128
5. Lu ZH, Macneil DD, Dahn JR (2001) *Electrochem Solid-State Lett* 4:A200. doi:10.1149/1.1413182
6. MacNeil DD, Lu ZH, Dahn JR (2002) *J Electrochem Soc* 149: A1332. doi:10.1149/1.1505633
7. Shaju KM, SubbaRao GV, Chowdari BVR (2002) *Electrochim Acta* 48:145. doi:10.1016/S0013-4686(02)00593-5
8. Shaju KM, SubbaRao GV, Chowdari BVR (2004) *J Electrochem Soc* 151:A1324. doi:10.1149/1.1775218
9. Zhang S, Qiu X, He Z, Weng D, Zhu W (2006) *J Power Sources* 153:350. doi:10.1016/j.jpowsour.2005.05.021
10. Park SH, Shin HS, Myung ST, Yoon CS, Amine K, Sun YK (2005) *Chem Mater* 17:6. doi:10.1021/cm048433e
11. Kim JM, Chung HT (2004) *Electrochim Acta* 49:937. doi:10.1016/j.electacta.2003.10.005
12. Li D, Muta T, Zhang L, Yoshio M, Noguchi H (2004) *J Power Sources* 132:150. doi:10.1016/j.jpowsour.2004.01.016
13. Liu ZL, Yu AS, Lee JY (1999) *J Power Sources* 81–82:416. doi:10.1016/S0378-7753(99)00221-9
14. Luo X, Wang X, Liao L, Wang X, Gamboa S, Sebastian PJ (2006) *J Power Sources* 161:601. doi:10.1016/j.jpowsour.2006.03.090
15. Zhang X, Wen Z, Yang X, Xu X, Li J (2006) *Mater Res Bull* 41:662. doi:10.1016/j.materresbull.2005.08.033
16. Zhang S (2007) *Electrochim Acta* 52:7337. doi:10.1016/j.electacta.2007.06.015